

**DESIGN AND DEVELOPMENT OF A 3.6 GHZ DIELECTRIC
RESONATOR OSCILLATOR WITH WIDE TUNING
SENSITIVITY.**

By

AMIR EFFENDY BIN MUHAMMAD AFIFI

**Thesis submitted in fulfillment of the requirements for the
Degree of Master of Science**

September 2011

ACKNOWLEDGEMENTS

All praises to Allah, unto Him belongs all the knowledge and understanding. I would like to acknowledge and extend my heartily gratitude to the following people without whom the completion of this research would not have been possible. I wish to express my appreciation and thankfulness to my supervisor, Dr. Widad Ismail who was very helpful and offered invaluable advice, support and guidance; not forgetting my initial supervisor, Dr. Mandeep Singh for his encouragement and advice that motivated me to take up this research. My appreciation to my manager, Lim Kok Keong, who shares the same admiration for knowledge and ‘technology’; for his persistent support in all my works. I would also like to convey thanks to Agilent Technologies for funding the materials in this research. To my colleagues Law Boon Wan, Toh Chee Leng and Ahmad Helmi Mokhtar for their relentless help and technical contribution, let me express my sincere gratitude. I wish to express my love and gratitude to my beloved wife, Alhan Farhanah, my children and family; for their understanding & sacrifice, throughout the duration of my study. I thank you to all of you and indeed Allah is the best for reward and the best for the final end.

TABLE OF CONTENTS

ACKNOWLEDGEMENTS	ii
Table of Contents	iii
LIST OF TABLES	vii
LIST OF FIGURES.....	ix
LIST OF SYMBOLS	xvii
ABBREVIATIONS.....	xix
ABSTRACT.....	xx
ABSTRAK.....	xxii
1 INTRODUCTION.....	1
1.1 Motivation – A High Tuning Sensitivity Second Down-Converter Local Oscillator.....	1
1.2 Research Problem Statement	1
1.3 Research Objectives	3
1.4 Research Scope and Limitations.....	4
1.5 Research Contribution.....	5
1.6 Thesis Organization	5
2 LITERATURES REVIEW	7
2.1 Microwave Frequencies Sources	7

2.2	Active Device Consideration for Oscillator	8
2.3	High Q-factor Resonator	11
2.4	Dielectric Waveguide as a Microwave Resonator	13
2.5	Discussion on DR tuning techniques prior works.....	14
2.6	Electrically Driven Tuning Options	15
2.6.1	Magnetic and Optic Tuning DRs	15
2.6.2	Varactor Diode.....	17
2.6.3	Varactor Tuned DRs	19
2.7	Literature Review Summary	30
3	DESIGN OF A DIELECTRIC RESONATOR OSCILLATOR.....	33
3.1	Dielectric Resonator Oscillator Specification	33
3.2	Development Flowchart	34
3.3	Dielectric Resonator.....	35
3.3.1	Resonant Mode	36
3.4	Resonance Structure Construction.....	38
3.4.1	Metal Enclosure Effect on Resonant Mode and Frequency	39
3.4.2	DR Coupling to Microstrip.....	43
3.4.3	Mechanical Adjustment of Resonant Frequency	46
3.4.4	Electronic Tuning Element – Varactor.....	47
3.4.5	Microstrip Stub Coupled Varactor Tuning – Tunable Resonant Circuit	53
3.5	Microwave Oscillator Fundamentals	56

3.5.1	Positive Feedback Oscillator	57
3.5.2	Negative Resistance Oscillator	59
3.6	Phase Noise Consideration	61
3.6.1	Active Device Selection – Bipolar Junction Transistor	63
3.7	Reference Dielectric Resonator Oscillator Design	64
3.7.1	Gain Block Design for Positive Feedback Oscillator	64
3.7.2	Integration of the Gain Block and the Feedback Block	66
3.8	Chapter 3 Summary	66
4	SIMULATIONS, MEASUREMENTS AND EXPERIMENTS TO IMPROVE DRO K_V	67
4.1.1	Amplifier Matching for Gain and Open Loop Phase Shift	67
4.1.2	Phase Noise	72
4.1.3	Tunable Resonance Structure Coupling to Amplifier Block	73
4.1.4	Signal Coupling to Output	75
4.2	Initial DRO Performance	77
4.2.1	Fundamental Frequency and Tuning Sensitivity	77
4.2.2	Power & Harmonics	80
4.2.3	Phase Noise	82
4.3	Analysis and Experiments to Improve DR Tuning Bandwidth	83
4.4	Investigating the Effect of Tuning Stub Dimensions on Resonant Structure Tuning Bandwidth.	91
4.4.1	$TE_{01\delta}$ H-field Pattern in the Resonant Structure	92

4.4.2	Tunable Resonant Structures Frequency Response Simulations.....	97
4.5	Validating the New DRO Functionality.....	98
4.5.1	Realization of a Negative Resistance Oscillator Alternative	99
4.5.2	Modification of Tunable Resonant Structure (vi).....	101
4.6	Chapter 4 Summary.....	103
5	RESULTS AND DISCUSSION OF THE PROPOSED DRO	104
5.1	Negative Resistance DRO Performance.....	104
5.2	Comparison with Prior Works and Researches	108
5.3	Chapter 5 Summary.....	115
6	CONCLUSION AND FUTURE WORKS	116
6.1	Conclusion on the High K_V and Wide Tuning Range DRO Design.....	116
6.2	Future Work on the High K_V DRO	117
6.2.1	Phase Noise Improvement	117
6.2.2	Further K_V or Tuning Range Improvement for Cost Reduction Opportunity	118
	LIST OF PUBLICATIONS	120
	APPENDIX A.....	121
	APPENDIX B	122
	APPENDIX C	123
	APPENDIX D.....	124
	APPENDIX E	125
	REFERENCES	126

LIST OF TABLES

		Page
Table 2.1	Summary of prior works that achieved wide tuning bandwidth.	31
Table 3.1	Specification of the DRO.	33
Table 3.2	Overview of ceramic materials available for the dielectric resonator	35
Table 3.3	Off-the-shelf metal enclosure dimensions	40
Table 3.4	Calculated waveguide resonant wavelength, $\lambda_d/2$ for available materials (Trans-Tech 2003).	41
Table 3.5	Electrical properties of 4500 series dielectric resonator fabricated for this design, based on the manufacturer measurement.	42
Table 3.6	Fabricated dielectric resonator physical dimensions.	42
Table 3.7	Materials used in the gain block or amplifier construction.	65
Table 4.1	Antenna-waveguide structure simulation and measurement data.	76
Table 4.2	Summary of proposed tuning structures performance.	91

		Page
Table 5.1	Comparison of harmonics level between negative resistance oscillator and initial positive feedback oscillator.	106
Table 5.2	High KV negative resistance DRO specifications	108
Table 5.3	Summarized comparison between proposed DR tuning technique and related prior works.	114






LIST OF FIGURES

	Page
Figure 2.1 Q factors of some resonators used in microwave frequency circuits (Carter and Flammer 1960; Day 1970; Gopinath 1981; Plourde and Chung-Li 1981; Trans-Tech 2003; Gardner 2005; Mazierska, Krupka et al. 2006).	12
Figure 2.2 Optical tuning dielectric resonator with photoconductive semiconductor as part of tuning stub.	17
Figure 2.3 Varactor γ ; (a) abrupt junction and (b) hyperabrupt junction	18
Figure 2.4 Dielectric resonator resonant circuit with balance loop varactor tuning (El-Moussaoui, Kazeminejad et al. 1989).	20
Figure 2.5 Balanced loop varactor circuit (El-Moussaoui, Kazeminejad et al. 1989)	21
Figure 2.6 Varactor tuning with the tuning stub electrical length optimizable (Xiaoming and Sloan 1999).	24

		Page
Figure 2.7	Circular tuning stub proposed by Virdee (Virdee 1997), top view.	25
Figure 2.8	Popovic's tunable DR and resonant structure (Popovic 1990).	26
Figure 2.9	Multi-resonator DRO schematics, (a) parallel feedback and (b) series feedback configurations.	28
Figure 2.10	Complication in using multi-resonator DRO for wider tuning bandwidth.	29
Figure 3.1	A cylindrical DR with $TE_{01\delta}$ mode, (b) top view and (c) side view, in the case where $L < OD$ (Cohn 1968).	37
Figure 3.2:	(a) Microstrip, TEM mode (Gupta, Garg et al. 1996); (b) dielectric resonator $TE_{01\delta}$ resonant mode coupling to microstrip TEM mode; $\epsilon_2 \gg \epsilon_1$	44
Figure 3.3:	Electrical equivalent schematic circuit of the dielectric resonator coupling to a microstrip line.	45
Figure 3.4:	Initial stage breadboard circuit developed to characterize microstrip lines coupling to the dielectric resonator, dotted lines are indicating maximum H-field coupling points.	45

		Page
Figure 3.5	Simplified assembly of the DR resonant structure	47
Figure 3.6	BB857 diode capacitance (C_T) at 1 MHz versus the reverse voltage applied or the v_{tune} , taken from the datasheet (Infineon 2006).	49
Figure 3.7	ADS model of packaged BB857 constructed from its SPICE model and package model.	49
Figure 3.8	Simulation of packaged BB857 in ADS and EMDS at 1 MHz	52
Figure 3.9	Tunable resonant circuit assembly	55
Figure 3.10	Plot of the tunable resonant circuit simulated and measured transmission response (S_{21})	56
Figure 3.11	Positive feedback oscillator block diagram	57
Figure 3.12	Schematic of a positive feedback dielectric resonator oscillator	58
Figure 3.13	Equivalent circuit of a one port negative resistance oscillator	59
Figure 3.14	Negative resistance transistor oscillator	61
Figure 3.15	Leeson's model of feedback oscillator noise.	62

		Page
Figure 3.16	Typical oscillator phase noise spectra (Gardner 2005).	63
Figure 4.1	Layout of the amplifier circuit, the schematic is in APPENDIX D.	68
Figure 4.2	The amplifier gain and phase shift measurement setup.	68
Figure 4.3	The amplifier gain, the markers are showing the gain at 3.6 GHz.	69
Figure 4.4	The amplifier phase shift, the markers are phase shifts at 3.6 GHz.	70
Figure 4.5	Simulated and measured noise figure of the designed amplifier	71
Figure 4.6	The amplifier noise figure measurement setup.	71
Figure 4.7	Predicted phase noise for the designed oscillator	73
Figure 4.8	Measured response of the resonant structure described in section 3.4.5.	74
Figure 4.9	Complete oscillator circuit resting in bottom enclosure	75
Figure 4.10	Oscillator signal coupling to the output	77

	Page
Figure 4.11	Spectrum measurement set up. 77
Figure 4.12	DRO center frequency reading. 79
Figure 4.13	The positive feedback DRO f_0 versus v_{tune} . 80
Figure 4.14	Frequency spectrum of the dielectric resonator oscillator 81
Figure 4.15	Phase noise measurement using Agilent E5052B signal source analyzer 82
Figure 4.16	Dielectric resonator oscillator phase noise, measured and simulated. 83
Figure 4.17	Proposed tunable resonant circuit designs. 86
Figure 4.18	Frequency sweep (solid lines) and insertion loss (dotted lines) versus v_{tune} measurements for structure (i) –  , (ii) –  and (iii) –  , tuning ranges shown in percentage. 87
Figure 4.19	Frequency sweep (solid lines) and insertion loss (dotted lines) versus v_{tune} measurements for structure (iii) –  and (iv) –  , tuning ranges shown in percentage. 88

	Page
Figure 4.20	89
Frequency sweep (solid lines) and insertion loss (dotted lines) versus v_{tune} measurements for structure (iv) – \square , (v) – \triangle and (vi) – \diamond , tuning ranges shown in percentage.	
Figure 4.21	90
Frequency sweep (solid lines) and insertion loss (dotted lines) versus v_{tune} measurements for structure (vi) – \square and (vii) – \triangle , tuning ranges shown in percentage.	
Figure 4.22	93
Resonant structure model for EMDS simulations.	
Figure 4.23	96
Magnetic field patterns of the tunable resonant structures; (a), (b), (c) corresponds to structure (iv), (v), (vi) respectively.	
Figure 4.24	97
Frequency response simulations of the tunable resonant structures; solid lines are resonant frequencies and dotted lines are insertion loss.	
Figure 4.25	99
Negative resistance source implementation	
Figure 4.26	100
Simulated and measured negative resistance source return loss	

		Page
Figure 4.27	Smith chart showing impedances and reflection coefficients of negative resistance source (Z_{negR} , Γ_{negR}) and tunable resonant structure (Z_{DR} , Γ_{DR}).	101
Figure 4.28	Modified tunable resonant structure (vi) – a one port network	102
Figure 4.29	The negative resistance oscillator, housed in the same package as the previous positive feedback oscillator.	103
Figure 5.1	Measurement of the designed negative resistance dielectric resonator oscillator tuning range – solid line and power – dotted line.	105
Figure 5.2	Spectrum of the negative resistance dielectric resonator oscillator.	106
Figure 5.3	Phase noise of the two oscillators.	108
Figure 5.4	Tuning range of the negative resistance DRO (■, solid line) and the corresponding DR resonant circuit (◆, dashed line), i.e. structure (vi).	109
Figure 5.5	Experimental results of the optically-tuned dielectric resonator (Jianping and Deming 1998).	110

		Page
Figure 5.6	At distance of 4 mm from top cover, the balance-loop varactor circuit performance, tuning range = 3 MHz; resonant frequency (◆, solid line); Q factor (▲, dashed line) (El-Moussaoui, Kazeminejad et al. 1989).	111
Figure 5.7	Tuning range as a function of the balance-loop varactor circuit distance from the top cover; theory (◆, dashed line); experiment (■, solid line) (El-Moussaoui, Kazeminejad et al. 1989).	112
Figure 5.8	◆ - Resonant frequency, ■ - unloaded Q obtained using Virdee's tuning configuration (Virdee 1997).	113

LIST OF SYMBOLS

Γ	Reflection coefficient
λ	Wavelength in vacuum, free space or air
ω	Frequency in radian
β	Transistor current gain
ω_C	Resonant frequency in radian
λ_d	Guide wavelength
ϵ_r	Dielectric constant
$1/f$	Flicker noise
C_{res}	Dielectric resonator equivalent capacitance
C_T	Varactor capacitance
F	Noise figure
Φ	Varactor built-in potential
Δf_0	Instantaneous oscillation frequency
f_C	Resonant frequency
f_m	Baseband frequency, offset frequency
f_0	fundamental signal or carrier frequency
f_T	Transit frequency
G_A	Amplifier power gain
GaN	Gallium nitride
I_C	Collector DC current
k	Boltzmann constant, $1.3806503 \times 10^{-23} \text{ JK}^{-1}$
Ka	Referring to 18 – 27 GHz frequency band
K_V	oscillator tuning sensitivity or oscillator gain

L_{res}	Dielectric resonator equivalent inductance
L_T	Tuning stub equivalent inductance
N	Coupling coefficient (i.e. in transformer)
$P_{1\text{dB}}$	Output power 1 dB compression point
P_O	Output power
Q_L	Loaded Q
Q_U	Unloaded Q
T	Temperature (in Kelvin)
$\tan \delta$	Losses in the (dielectric) material
$TE_{01\delta}$	Transverse electric resonant mode in dielectric resonator
TE_{011}	Transverse electric resonant mode in cavity resonator
TE_{111}	Transverse electric resonant mode in cavity resonator
v_b	Base voltage
V_{CC}	Supply voltage, e.g. at collector
V_i	Input signal, in volt
V_o	Output signal, in volt
V_{tune}	Varactor bias, tuning voltage
V_{DC}	Instantaneous varactor tuning voltage
W_ϕ	Single sided noise spectral density

ABBREVIATIONS

ADS	Advanced Design System
BJT	Bipolar junction transistor
CW	Continuous wave
DC	Direct current
DR	Dielectric resonator
DRO	dielectric resonator oscillator
E-field	Electric field
EMDS	ElectroMagnetic Design System
FET	Field effect transistor
H-field	Magnetic field
IL	Insertion loss
LO	Local oscillator
PCB	Printed circuit board
PLL	Phase-locked loop
SA	Spectrum analyzer
SSA	Signal source analyzer
TEM	Transverse electric magnetic propagation mode
TWT	Travelling wave tube
UHF	Ultra high frequency
VCO	Voltage controlled oscillator
YIG	Yttrium-iron-garnet

DESIGN & DEVELOPMENT OF A 3.6 GHZ DIELECTRIC RESONATOR OSCILLATOR WITH WIDE TUNING SENSITIVITY.

ABSTRACT

An oscillator is required as a second stage LO in a superheterodyne SA. The oscillator operating frequency is a fixed 3.6 GHz, which is at the lower end of the microwave frequency range. There are several options of active devices and resonators that can be considered for the oscillator. A bipolar junction transistor (BJT) is chosen for the amplifier block due to its low flicker noise corner frequency and a dielectric resonator (DR) is chosen for its high Q factor. This combination yields a low phase noise oscillator. Apart from its high Q factor, a DR is a high dielectric constant ceramic thus enabling a miniaturized microwave oscillator design compared to a cavity resonator. A varactor-tuned technique is adopted because it results in a simple planar circuit design compared to optically and magnetically tune DR.

This dielectric resonator oscillator (DRO) must have very high frequency accuracy. The SA is specified to operate from 0°C to 55°C, thus among the design requirement for the DRO is to be operable in a wide temperature range and, to last for many, many years. Hence the DRO is controlled by a phase-locked loop (PLL). As the DRO signal drifts with temperature as well as due to aging, a wide tuning range is necessary to guarantee a reliable and repeatable performance over its operating life.

An existing DRO with a tuning range of 0.14% at of 3.6 GHz was used as a benchmark. The development of the new DRO began with investigation on several proposed varactor-tuned DR resonant structures. The resonant structures were

observed for the resonant frequency tuning range, the linearity of resonant frequencies versus tuning voltages and the tuning sensitivity. The promising DR resonant structures – with wide tuning range, linear response and high tuning sensitivity, were further analyzed to understand the resonant structures coupling mechanism as well as the potential effect on the DRO performance like phase noise. The successful DR resonant structure combined with the BJT amplifier circuit formed the DRO. The first DRO is a positive feedback oscillator; however due to the resonant structure high insertion loss compared with the available amplifier gain, the DRO failed to work. An alternative negative resistance oscillator was then developed, also using the same model BJT. It worked based on signal reflection between the resonant structure port and the BJT emitter junction which posed a negative real impedance; it proved successful. The newly developed negative resistance DRO performance was measured and compared with the benchmark DRO. The new DRO yields a tuning range of 23 MHz or 0.65% at 3.6 GHz and a tuning sensitivity of 2.3 MHz/V. However, the new DRO phase noise degraded by about 10 dB compared with the benchmark DRO.

REKABENTUK & PEMBANGUNAN LITAR AYUNAN PENALA DIELEKTRIK 3.6 GHZ DENGAN KEPEKAAN MENALA YANG LEBAR.

ABSTRAK

Sebuah pengayun diperlukan sebagai pengayun setempat peringkat kedua di dalam sebuah penganalisa spectrum superheterodyne. Frekuensi tunggal pengoperasian pengayun ini ialah 3.6 GHz, yang mana terletak di hujung rendah julat frekuensi gelombang mikro. Terdapat beberapa pilihan peranti aktif dan penala yang boleh dipertimbangkan untuk pengayun tersebut. Transistor dwikutub (BJT) dipilih untuk blok penguat kerana frekuensi sudut hingar kelipannya ($1/f$) yang rendah dan penala dielektrik (DR) dipilih kerana faktor Q' nya yang tinggi. Gabungan ini menghasilkan pengayun yang rendah hingar fasa. Selain dari faktor Q' nya yang tinggi, DR ialah seramik berpemalar dielektrik tinggi, jadi ia membolehkan pengecilan rekabentuk pengayun gelombang mikro berbanding dengan penala berongga. Teknik talaan-varaktor digunakan supaya rekabentuk litar yang rata dan ringkas dapat dihasilkan berbanding DR talaan optik atau magnet.

Pengayun penala dielektrik (DRO) ini wajib mempunyai ketepatan frekuensi yang tinggi. Spesifikasi SA menetapkan pengoperasian dari 0°C hingga 55°C, oleh itu antara keperluan rekapipta DRO ini ialah kebolehan beroperasi dalam julat suhu yang lebar dan bertahan untuk bertahun-tahun lamanya. Oleh sebab itulah DRO ini dikawal oleh lingkaran fasa-berkunci (PLL). Oleh kerana isyarat DRO boleh tersasar mengikut perubahan suhu dan juga akibat penuaan jangka hayat, maka, julat talaan yang lebar adalah satu keperluan untuk memastikan prestasi yang terjamin setiap kali, sepanjang hayat pengoperasiannya.

Sebuah DRO sedia ada dengan julat talaan sebanyak 0.14% pada 3.6 GHz telah digunakan sebagai penanda aras. Pembangunan sebuah DRO yang baru bermula dengan kajian ke atas beberapa cadangan struktur talaan DR yang ditala-varaktor. Pemerhatian dilakukan ke atas julat penalaan frekuensi, kelurusan frekuensi talaan lawan voltan menala dan kepekaan menala. Struktur talaan DR yang berpotensi – dengan julat menala yang lebar, respons yang lurus dan kepekaan menala yang tinggi, dianalisa selanjutnya untuk memahami mekanisma gandingan struktur talaan dan juga kesan yang berkemungkinan ke atas prestasi DRO seperti hingar fasa. Struktur talaan DR yang terpilih digabungkan dengan litar penguat BJT, seterusnya membentuk sebuah DRO. DRO yang pertama ialah sebuah pengayun suapbalik positif, walau bagaimanapun, akibat kehilangan sisipan (IL) struktur talaan yang tinggi berbanding dengan gandaan penguat yang ada, DRO tersebut gagal berfungsi. Sebagai ganti, sebuah pengayun rintangan negative dibangunkan, menggunakan model BJT yang sama. Ia berfungsi berasaskan kepada pemantulan isyarat di antara liang struktur talaan dan simpang pemancar BJT yang menunjukkan galangan nyata negatif; ia terbukti berjaya. Prestasi DRO rintangan negatif yang baru dibangunkan ini diukur dan dibandingkan dengan DRO penanda aras. DRO yang baru membuahkan julat menala sebanyak 23 MHz atau 0.65% pada 3.6 GHz dan 2.3 MHz/V kepekaan menala, dengan voltan menala dari 0 – 10 V. Walau bagaimanapun hingar fasa DRO baru ini merosot lebih kurang 10 dB berbanding DRO penanda aras.

1 INTRODUCTION

There are many microwave frequency oscillators in the market serving the ever growing electronic communications. Most of the shelf devices are tailored to the commercial applications like mobile phones, wireless broadband data and broadcasting industries. Although there are suppliers that do custom designs for unique applications or low volume market, they come with high price tags; hence the need for in-house designs. Secondly, proprietary technologies are best kept with in-house design.

1.1 Motivation – A High Tuning Sensitivity Second Down-Converter Local Oscillator

A swept signal spectrum analyzer (SA) requires a fix frequency oscillator operating at 3.6 GHz for its second down-converter block. Although there is probably an application out there that works at 3.6 GHz, a tight requirement on this oscillator, as the SA is a test and measurement instrument, means the available of-the-shelf oscillator may not meet the requirement – electrical and mechanical specifications as well as physical size (form, fit and function). The SA is specified to operate over a wide temperature range i.e. from 0°C to 55°C and over a long period of time. Thus the oscillator frequency may drift over temperature as well as over time. Therefore, the oscillator requires a tuning mechanism for the frequency drift compensation; the frequency correction will be controlled by a PLL.

1.2 Research Problem Statement

In microwave fixed frequency oscillators as well as microwave filters, some limited tuning capability is necessary for center frequency adjustment. Dielectric resonator

materials have some fabrication tolerance which results in resonant frequency variation. This problem is commonly addressed by means of mechanical adjustments. However this is a onetime adjustment during manufacturing and it cannot correct the resonant frequency should there be drifts throughout the device operating life. A broad frequency range electronically tuned method as proposed in this research offers a solution to alleviate this problem. It should be applicable either in dielectric resonator oscillators and filters.

As for filters, particularly band pass filters, apart from the problem discussed above, having an electronic tuning capability allows for bands selection. I.e. instead of designing a broad band filter that covers the whole frequency channels, a narrower band pass filter could be designed which may improves adjacent channel rejection. The filter can be controlled to ‘pass’ only the channels it is operating.

The subsequent problem which will be the focus of this research is an example where a broad, electronically tuned capability is required. The SA second local oscillator specification requires a tuning bandwidth of 10 MHz and tuning sensitivity, $K_v = 1 \text{ MHz/V}$) to enable the oscillator to provide a reliable and consistent fixed 3.6 GHz signal to the down converter mixer in the SA. The output power for the 3.6 GHz signal is $+3 \text{ dBm} \pm 1 \text{ dB}$. Physically, the oscillator must be small enough to fit in a typical bench top SA.

Looking at the frequency and output power requirement as well as the size, a solid state oscillator is the most sensible option. With the choice of resonators available a planar circuit is feasible. For a low phase noise oscillator design; the solid state active device choice, e.g. a transistor or a diode must consider the flicker noise; and secondly a high Q-factor resonator (Gardner 2005). The temperature coefficient of the resonator resonance frequency must have a low part per million (p.p.m.) number

for stability over wide temperature range. Materials selection will be further discussed in the following sections.

1.3 Research Objectives

Based on the defined problem statement, the objectives of the research can be defined as follows:

- (i) To design a dielectric resonator oscillator (DRO) that must achieve a tuning bandwidth of at least 10 MHz with tuning voltage of 0 V to +10 V.

The main objective of this design is to establish a circuit technique that can achieve the wide tuning bandwidth; the choice of materials like transistor, resonator and varactor are secondary. In this study, a method for achieving wide tuning bandwidth and high tuning sensitivity, K_V for DRO will be investigated and verified with a final design of the DRO.

- (ii) To fabricate and measure the proposed DRO design that considers the need for it to suit manufacturing requirement

The solution is using low cost, off-the-shelf components; manufacturable with existing industrial technology e.g. printed circuit board (PCB) in mass production environment.

- (iii) To analyze and validate the performance of the proposed DRO for practical oscillator application and finalized the specification of such DRO in which, the tuning sensitivity must be linear to ease PLL control.

This study only focuses on the design of the wide tuning bandwidth DRO.

1.4 Research Scope and Limitations

The scope of this study is to find an electronically-tuned technique; that yields a wide tuning bandwidth for a passive dielectric resonator (DR) circuit and subsequently apply it to a DRO design and test the DRO functionality. The activities include:

1. Literatures review on microwave signal sources, DR technologies, related materials and devices to construct microwave oscillators and prior works and techniques on DROs;
2. Characterize a DR circuit and the corresponding DRO (previously developed by the author) to be used as a reference for the prospective oscillator,
3. Simulation of several initial proposed passive DR circuits, fabrication of the designed circuits and measurements of the circuits.
4. Promising circuits will be further analyzed to find a trend that will give a wide tuning bandwidth. Finally the passive circuits will be adopted into DRO designs to prove the technique effectiveness.

This research does not intend to include in-depth study and improvement on phase noise for the prospective DRO; however phase noise performance of the ‘reference’ and ‘prospective’ oscillators will be measured for completeness.

In the design, especially in simulation related to non-linearity parameters like the amplifier gain and its open loop phase; reflection coefficient of negative resistance port are not very correlated to their corresponding measurements. This is due to limitation to components non-linearity parameters in the models in particular the transistor.

Circuit fabrication accuracy is as good as the prototyping machine capability, hence some losses in measurements that are unaccounted for in simulations like insertion loss and amplifier gain. The three dimensional electromagnetic field simulator, EMDS, uses a lot of computer resources. Additional components used in supporting measurement like RF SMA connectors are not included in the three dimensional electromagnetic field simulation to reduce model complexity.

1.5 Research Contribution

This research proposes a technique to increase DRO tuning range with high tuning sensitivity; suitable where only small v_{tune} range is available. The technique offers a low impedance varactor tuning stub that couples to the DR, exploiting the DR TE_{018} resonant mode. It is a practical approach where mass production is intended as most of the components to build the circuit, are available off the shelf. Minimal custom-made components are necessary, which are unique to the desired operating frequency such as the metal enclosure, the DR and the PCB, of course. The technique is also applicable for DR filter application as stated earlier in Section 1.2.

1.6 Thesis Organization

This introductory chapter presents the background of the problem that leads to this research and development on the prospective DRO. This is followed by objectives of the study and the expected end results.

The following literature review chapter begins with a brief review of microwave sources technologies currently available, related materials and devices to construct microwave oscillators and how the selection of materials relates to the theory, some

fundamentals on DR applications followed by discussion on DROs prior works and techniques.

In chapter 3, the research flowchart is presented. From here the proposed passive tunable resonant circuits and experiments will be laid out to find out a tunable circuit that is promising for a wide tuning bandwidth. Finally a brief notes on oscillator fundamentals.

In Chapter 4 the analysis and results from all experiments are presented and analyzed in determining a tunable circuit that can yield a wide tuning bandwidth. The second part of this chapter elaborates how a potentially wide tuning bandwidth resonant circuit is designed into a DRO. The potential wide tuning bandwidth DRO design presented in Chapter 4 is further discussed in Chapter 5, in comparison with existing and prior works or reports.

Finally the study's findings is discussed and summed up; and in particular in the justification of adopting the design in the said application as well as other potential applications. Potential future works would also be discussed in which how to possibly improves the phase noise, an important figure of merit for an oscillator and secondly the possibilities to further increase the tuning range and/or tuning sensitivity, K_V .

2 LITERATURES REVIEW

In general, microwave frequency signal sources are either wide band and tunable like YIG-tuned oscillators, voltage controlled oscillators and frequency multipliers; or fixed frequency like coaxial resonator oscillators and DROs. Although categorized as fixed frequency, coaxials and DROs do have limited tunability for frequency correction. The categories only imply the oscillators' applications. A microwave oscillator (wide band or fixed frequency) is basically a high Q-factor resonator with an appropriate coupling structure, couples to an active device.

2.1 Microwave Frequencies Sources

Microwave frequencies range from 300 MHz to 300 GHz, i.e. equivalent to wavelength of one meter down to one millimeter respectively (Pozar 1998). This is a broad definition that includes ultra high frequencies (UHF) all the way to millimeter waves. Commonly, microwave frequencies usually refer to 3 GHz to 30 GHz, or 10 cm to 1 cm wavelength at minimum, however in RF engineering the lower boundary is usually at 1 GHz (30 cm), and the upper around 100 GHz (3 mm).

Microwave sources have different types of constructions and unlike lower frequencies, are not limited to PCB. Vacuum tube devices include the magnetron, klystron, traveling-wave tube (TWT), and gyrotron, and operate on the ballistic motion of electrons in a vacuum under the influence of controlling electric or magnetic fields. Vacuum tube devices are cumbersome but are capable of very high output power, for example a continuous wave (CW) helix TWT yields an output power in the range of several kilowatts at X band (Coaker and Challis October 2008). A 'microwave amplification by stimulated emission of radiation' (maser)

produces coherent electromagnetic waves through amplification due to stimulated emission; it has a very high frequency precision (Calosso, Levi et al. 2005). Solid-state sources can be constructed from bipolar junction transistors (BJT), field-effect transistor (FET) – at high microwave frequencies, tunnel diodes, Gunn diodes, and IMPATT diodes. Solid state microwave oscillators are relatively smaller in size than the above two sources; and can be either planar circuits i.e. on PCBs or combination of planar circuits and physical structures, depending on the choice of resonators. Until recently, solid state devices are capable of low to medium power handling in microwave applications. With the advent of GaN devices, wideband capability (ABI-Research 2009) and high power applications are possible all way into Ka band (Shealy, Smart et al. 2002). Such prospect combined with lower cost gives microwave solid state oscillators a promising future.

2.2 Active Device Consideration for Oscillator

An important parameter for any oscillators is its signal purity. As for harmonics, if any of the harmonics signal is too high, it could cause the PLL to lock on that harmonic instead of the fundamental signal, f_0 ; secondly it could also create a spurious signal at a mixer output like the one this oscillator is intended for. A low pass filter can be added at the output of the oscillator to suppress the harmonics. The harmonics arise due to the active device non-linearity. To reduce the harmonics power level, the device must have much higher P_{1dB} than the required output power for the f_0 .

For phase noise, the active device must have low $1/f$ noise (or the flicker noise) because this noise is up converted to the sideband of the oscillator output signals. BJT has large parasitic capacitance to the ground, resulting in reduction of the $1/f$

noise. Also, $1/f$ noise is directly proportional to the current density in the transistor. Large transistors with high maximum collector current, when used at low currents will give the best $1/f$ performance. Harmonics can mix $1/f$ noise up and mix back to the fundamental signal – this would cause higher phase noise. Choosing BJT with low f_T , means less harmonics generated and thus lower phase noise. A simple guideline is the device f_T should be two or three times the operating frequency (Muat 1984). FET devices although they too can offer high P_{1dB} , unfortunately have higher $1/f$ corner frequency. A typical submicron MOSFET device, with a bias current of several hundred microamperes would show a $1/f$ corner frequency around 1 MHz; and this is worse than BJT (Razavi 1997; Zhaofeng and Jack 2001). FET would be considered for oscillators operating beyond 10 GHz if the phase noise is not demanding as there aren't many BJTs available for operation above 10 GHz. Now with the presence of heterojunction bipolar transistors (HBT), the bipolar transistor technology is making its way even beyond 20 GHz as demonstrated by (Madhihian and Takahashi 1991); the HBT phase noise performance is either better (Ali Khatibzadeh and Bayraktaroglu 1990; Leier 2006) or comparable to BJT.

Gunn diodes are applied mostly in higher microwave frequencies i.e. 10 GHz onwards because the Gunn diode oscillators require cavity resonators, many works discussed oscillator applications in millimeter waves for example (Ruttan 1975; Rahal and Bosisio 1995; Priestley, Newsome et al. 2002), and an oscillator at 35 GHz presented by (Strangeway, Ishii et al. 1988) has quite low phase noise too e.g. -132 dBc/Hz to -125 dBc/Hz at 100-kHz offset from f_0 . Though theoretically it is possible to use the Gunn diode in this work, the cavity resonator size at 3.6 GHz makes it impractical for miniaturization. The cavity resonator will be further explained in the following section. Until recently, for many Gunn diode oscillators,

the frequency tuning is realized by the Gunn diode DC bias adjustment to create frequency pushing, this will complicate the design (Priestley, Newsome et al. 2002). Nowadays though, there are varactors offered for Gunn diode oscillator applications, like those offered by e2v Technologies (e2v 2008). IMPATT diodes are similar to Gunn diodes though they are not interchangeable. Their DC operating current is typically in hundreds of milliamps with output power ranges from tens to hundreds of milliwatts.

There are microwave voltage controlled oscillator (VCO) designs (Sheng-Lyang, Huang et al. 2008; Jhe-Jia, Zuo-Min et al. 2009) on integrated circuit (IC) for tunable oscillator applications with tuning range in hundreds of Megahertz to a few Gigahertz. Phase noise of tunable oscillator will suffer degradation due to the presence of a tuning element like varactor; and the wider the tuning bandwidth the poorer the phase noise (Carey 2011). Bulk acoustic wave (BAW) resonator oscillator is also an IC based but it is for a fixed frequency or narrow band application. For technological reasons BAW-based oscillators are limited up to 2 GHz (Li, Seok et al. 2011) though there are works (Aissi, Tournier et al. 2006; Li, Seok et al. 2011) showing BAW-based oscillators at higher frequencies, achieved by some sort of frequency multiplication. For a unique application i.e. this 3.6 GHz oscillator, an integrated circuit VCO would require a substantial financial investment.

Of all the choices of solid state devices mentioned above, discrete BJT is the most suitable for low noise design especially for low microwave frequencies; in fact Regis et al stated clearly their choice of BJT in (Regis, Llopis et al. 1998) for their ultra low phase noise oscillator; and Warburton for his 3 GHz oscillator (Warburton

2005). Considering cost, an off the shelf component is preferred over a dedicated IC designed oscillator.

2.3 High Q-factor Resonator

There are many choices of microwave resonators available for application in the S-band. Among others are cavity resonator (Condon 1941), yttrium-iron-garnet (YIG) crystal (Carter and Flammer 1960), dielectric resonators (Plourde and Chung-Li 1981) – both transverse electric magnetic (TEM) mode (coaxial resonator) and $TE_{01\delta}$ mode, and microstrip resonators to name a few. Among these resonators, microstrip resonators have the lowest Q factor which ranges in a few hundred (Gopinath 1981; Mazierska, Krupka et al. 2006) and they suffer from radiation loss due to their construction on low dielectric constant substrates (Belohoubek and Denlinger 1975). The cavity resonator must be designed to resonate in TE_{011} mode instead of at the dominant cylindrical cavity mode, TE_{111} , at 3.6 GHz in order to achieve higher Q (Pozar 1998). For this, its radius and height are approximately 5.5 cm and 11 cm respectively, which are rather bulky and furthermore the structure is made of metal, the dimensions tend to change with temperature.

YIG is a ferrimagnetic material that exhibits ferrimagnetic resonance. A YIG crystal in sphere shape when subjects to a DC magnetic field (H-field) and placed in an RF structure, exhibits a high Q resonance at a microwave frequency proportional to the DC H-field. The resonance frequency is tunable a few octave range by varying the DC H-field and there is a minimum DC H-field required depends on the YIG saturation magnetization value. The YIG sphere is only a few tens of mils in size but the solenoid structure that provides the DC H-field is cumbersome and that, this design is focus on a fix frequency oscillator and does not require a few octave of

tuning range. Figure 2.1 summarizes the Q factors of common and commercially available resonators used in microwave frequency circuits.

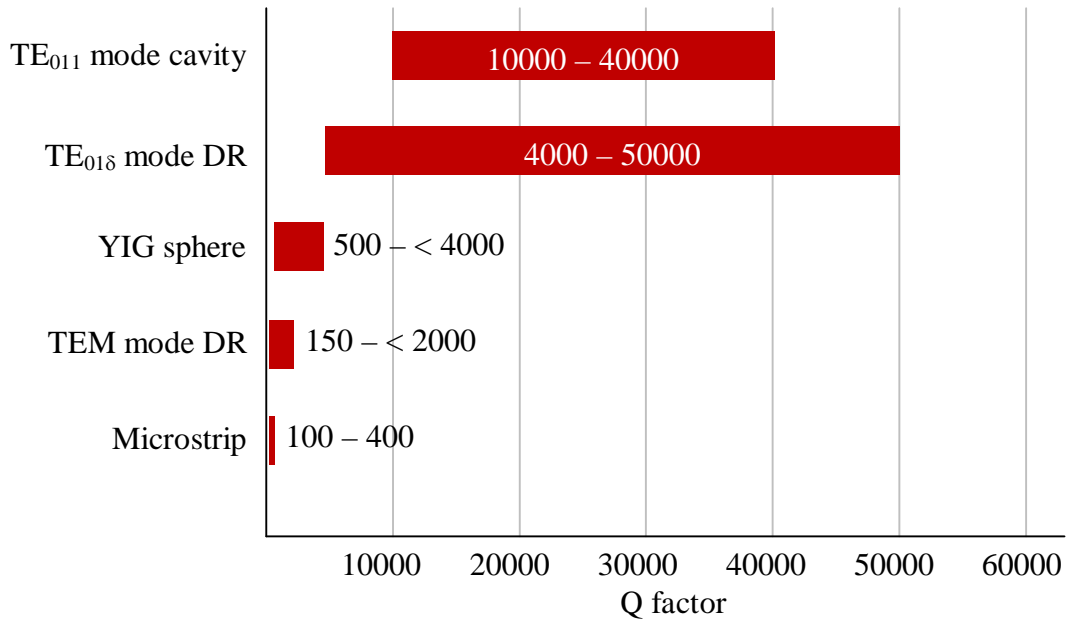


Figure 2.1: Q factors of some resonators used in microwave frequency circuits (Carter and Flammer 1960; Gopinath 1981; Trans-Tech 2003; Gardner 2005; Yom, Shin et al. 2005; Mazierska, Krupka et al. 2006; Yom, Shin et al. 2007).

The two possible candidates left are either TEM mode coaxial resonator or TE_{01δ} mode DR. In terms of size they both are reasonably small though coaxial resonator is smaller than the later. However, in general the TE_{01δ} mode DRs possesses a much higher Q i.e. in the range of thousands whereas the coaxial resonators Q are in the range of a few hundreds.

The TE_{01δ} mode DR material is a titanate based ceramic and will be used in the design because of its excellent frequency stability over temperature and over time. The high Q-factor is due to the ceramic material inherently very low loss i.e. $\tan \delta$ (Fiedziuszko, Hunter et al. 2002); an important feature for short term frequency

stability or phase noise (δ is the loss angle from $\tan \delta = \varepsilon'' / \varepsilon'$, and ε is the electrical permittivity). Else the DRO would require a much wider tuning bandwidth and possibly the PLL must have a relatively faster lock time or wider loop bandwidth which could potentially degrade the far-out phase noise.

2.4 Dielectric Waveguide as a Microwave Resonator

Guided electromagnetic wave propagation in dielectric structures have been discovered as earlier than 1920. In 1935 G. C. Southworth received U.S. Patent 2106769 describing, “The wave guiding structure may take a variety of forms: a typical guide consists of a rod of dielectric material having high dielectric coefficient relative to unity”. “A specific dielectric guide which may be considered is a cylinder of ceramic material having rutile (titanium dioxide) as its principal constituent” (Southworth 1935). In 1939 Richtmyer showed that unmetallized dielectric materials can perform as electrical resonators and he termed dielectric resonators (Richtmyer 1939).

In their paper, Okaya and Barash presented the first analysis on high dielectric materials resonant frequency, modes and DR circuit design (Okaya and Barash 1962). However due to temperature instability – variation of dielectric constant over temperature, of the early high dielectric constant materials like rutile, they don’t find practical usage (Fiedziuszko, Hunter et al. 2002). Finally in 1970s the first temperature stable ceramic, barium tetratitanate was developed by Raytheon (Masse, Pucel et al. 1971). This paved the way for DRs applications in microwave frequencies. Later on, composite DRs with high dielectric constant and adjustable temperature coefficients were introduced (Wakino, Nishikawa et al. 1975) allowing for more commercial applications.

Energy is confined in a dielectric waveguide by total internal reflection mechanism whereby a core dielectric material with higher index of refraction is surrounded by dielectric material with lower index of refraction (Snitzer 1961) e.g. air. The DR has very small, finite loss tangent ($\tan \delta$) and no wall losses in the dielectric, hence the high unloaded Q, this is given by $Q_u = 1/\tan \delta$; especially true for high dielectric constant e.g. 100 or more. The electric field decays exponentially outside the resonator. The resonant frequency depends on the dielectric constant (ϵ_r), the dimensions and the shape of the resonator (Okaya and Barash 1962; Cohn 1968). Some common application of high dielectric constant materials are band-pass filters, dielectric antenna, DROs and ferroelectric devices (Fiedziuszko, Hunter et al. 2002).

2.5 Discussion on DR tuning techniques prior works

Many papers have proposed various means of tuning the DR, and most papers (El-Moussaoui, Kazeminejad et al. 1989; Krupka 1989; Buer and El-Sharawy 1995; Virdee 1997; Xiaoming and Sloan 1999; Alford, Petrov et al. 2002) discuss their proposals based on DR resonant circuits as examples rather than explicitly on DROs. This is understandable due to the fact that microwave DROs constructions are basically a DR resonant circuit coupling to an active device circuit like a transistor or a Gunn diode. The resonant circuits can also be the construction blocks for band pass filters.

With regards to the oscillator construction, a standalone resonant circuit that promises the desired tuning specifications – Q factor, range and sensitivity, will not necessarily achieve the same tuning characteristics when connected as an oscillator. For example the Q factor, a standalone resonant circuit would have a high loaded Q (Q_L) but when coupled to an active device circuit which would have different

impedances at its ports; will create a mismatch and loss to the overall circuit. This results in the Q_L being degraded.

Thus it is important too, to validate a promising DR resonant circuit with an oscillator example. The literature review will nevertheless discuss the prior works which are mostly on DR resonant circuit examples. Many DRO examples (Ishihara, Mori et al. 1980; Kharkovsky, Kirichenko et al. 1996; Yom, Shin et al. 2007) don't emphasize on wide tuning range and high tuning sensitivity which on the contrary is the main objective of this work.

2.6 Electrically Driven Tuning Options

DR is tuned effectively by perturbing its electromagnetic fields in the excited resonant mode. The perturbation can be achieved mechanically and electrically. The interest in this work is on electrically excited perturbation given the application of the DR resonant circuit as an oscillator controlled by a PLL. Several widely known electrical tuning techniques by means of magnetic, varactor, and optic are discussed in these article (Virdee 1998) and paper (Farr, Blackie et al. 1983).

2.6.1 Magnetic and Optic Tuning DRs

Magnetically tuned DR is realized by attaching a microwave ferrite material to the resonator. H-field which is usually provided by solenoid is applied to the ferrite to control its magnetic property. This is a current controlled tuning system. Krupka, in his paper (Krupka 1989), proposed putting a ferrite rod co-axis with the DR disc. He achieved a very high tuning bandwidth of 120 MHz on his magnetically tuned resonant system, considering the hysteresis in magnetic structure. Otherwise, with a completely demagnetized ferrite to the maximum applied H-field, he achieved 405 MHz tuning range ($\approx 4\%$). The downside of this magnetically tuned system is the

slow tuning speed, as Krupka also hope to obtain a faster tuning speed. Secondly the electromagnetic structure that provides the H-field for his system is bulky, i.e. the diameter of the electromagnetic poles is 250 mm. In fact this is typical drawback of electromagnetic structures for similar applications. This negates the advantage of DR for miniaturization.

Interest in optically tuned DR arises because the technique offers high isolation between the tuning DC bias and the radio frequency (RF) signals, and potentially very wide bandwidth. The first method, a photoconductive semiconductor slab is attached on top of the DR cylinder. A light from a diode or a laser illuminates the semiconductor slab thus creating a plasma layer on the slab illuminated surface. The plasma behaves like a conductive tuning plate and the amount of frequency shift depends on the plasma density, which is proportional to the illumination intensity (Shen, Nickerson et al. 1993). Another optical method proposes putting a photoconductive semiconductor patch as part of microstrip tuning stubs as shown in Figure 2.2. The tuning stubs add reactance to the DR, whereby the photoconductive patch connects the two stubs. By varying the light intensity illuminating the photoconductive patch, the overall reactance of the resonator circuit is altered. Thus the resonant frequency of the DR is tuned (Jianping and Deming 1998). This method achieves a very much wider tuning range as oppose to the former (Shen, Nickerson et al. 1993); both using Silicon (Si) as the photoconductive material for tuning at X-band in their experiments.

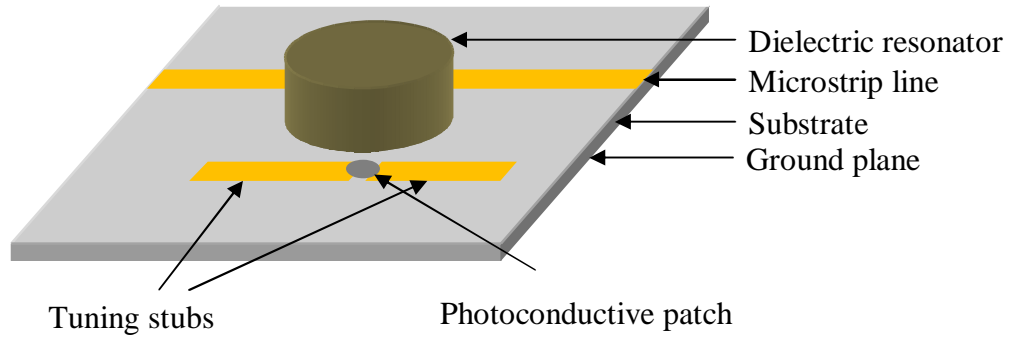


Figure 2.2: Optical tuning dielectric resonator with photoconductive semiconductor as part of tuning stub.

Despite the achievement and advantages of the optical tuning techniques, the fact that a light source has to be inserted means the DR metal enclosure has to have an opening for the light source. This will potentially cause some loss to the radio frequency signal as well as external interference. For this research, having to add a light source is not favorable as it is more complex as compared to the varactor tuning techniques that will be discussed in the following section.

2.6.2 Varactor Diode

Varactor or variable capacitance diode enables fast electronic tuning and it achieves this without any physical movement. There are two type of varactors based on the doping structure introduced inside the semiconductor. An abrupt diode has the doping structure such that its gamma, γ is about 0.47, for a practical diode (Klymyshyn, Kumar et al. 1997); where γ is the slope of the curve $\log(\text{varactor capacitance}, C_T)$ versus $\log(v_{\text{tune}} + \Phi)$; v_{tune} is the varactor bias voltage and Φ is the varactor built-in potential, this is depicted in Figure 2.3. A hyperabrupt diode has the

doping structure such that its $\gamma > 0.5$ (Frazier 1959; Covington and Hicklin 1978). For varactors considered for this research, the abrupt junction diodes capacitance ratio (capacitance at minimum v_{tune} /capacitance at maximum v_{tune}) is typically about 4 (Khanna 1987) and the hyperabrupt junction diodes, is > 10 (Infineon 2006). In other words, the hyperabrupt junction varactor will give bigger tuning range compared to the former. Al-Charchafchi and Dawson developed a varactor-tuned ring resonator with a wide tuning bandwidth, of 31% at 3 GHz using a hyperabrupt junction varactor (Al-Charchafchi and Dawson 1989). Hence for this research, the hyperabrupt junction varactor will be used. However, γ for hyperabrupt junction varactors may not be constant over the v_{tune} range. For that reason, for a limited range of v_{tune} the γ can be assumed constant.

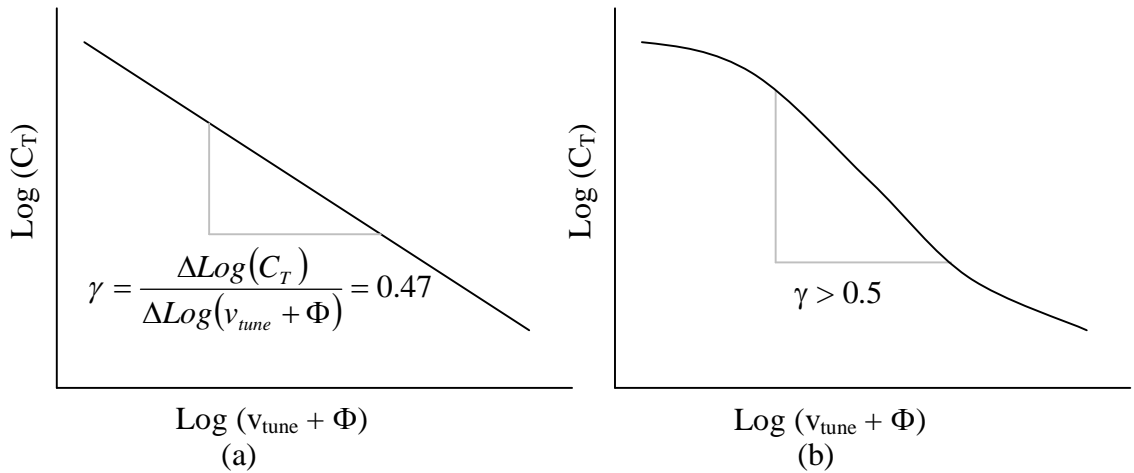


Figure 2.3: Varactor γ ; (a) abrupt junction and (b) hyperabrupt junction

Adding an electronic tuning element like varactor is not without a cost. When the varactor is biased at a particular v_{tune} , the resulting RF signal in the resonant circuit causes a jittery v_{tune} . The jittery v_{tune} translate into phase noise on the RF signal

(Carey 2011). Consider an oscillator with a tuning sensitivity K_V and tuning voltage v_{tune} . The oscillation frequency, f_0 is

$$f_0 = f_{00} + K_V v_{\text{tune}} \quad 2.1$$

Where f_{00} is the oscillation frequency at $v_{\text{tune}} = 0$ V.

At a particular $v_{\text{tune}} = V_{\text{DC}}$, the presence of RF signal in the resonant circuit causes jitter to v_{tune} and is assumed to vary as such;

$$v_{\text{tune}} \approx (V_{\text{DC min}} + V_{\text{DC max}}) / 2 \quad 2.2$$

And thus the range of the instantaneous oscillation frequency, Δf_0 is

$$\Delta f_0 = K_V (V_{\text{DC max}} - V_{\text{DC min}}). \quad 2.3$$

The Δf_0 appears as the sideband spectrum of the oscillation frequency and is observed as the phase noise due to the varactor function.

2.6.3 Varactor Tuned DRs

In varactor tuned resonant circuit, looking from lump elements circuit model, the varactor capacitance (C_T) is the variable reactance that is added to the resonator (parallel R_{res} , L_{res} , C_{res}) and thus varies the resonant frequency. The papers discussed in this section explain how the varactor is coupled to the DR and thus form the tunable DR circuit. In summary, the varactor reactance coupling to the DR is by means of the H-field when the DR is excited in $\text{TE}_{01\delta}$ resonant mode as depicted in Figure 3.1.

2.6.3.1 Balanced Loop Varactor Circuit

El-Moussaoui et al proposed a balanced loop varactor circuit (El-Moussaoui, Kazeminejad et al. 1989) where the varactor loop is mounted above the DR as shown in Figure 2.4 below. The loop uses two varactors and is wound in opposite

direction to cancel the loop inductance and consequently prevents the varactor loop from resonating with the DR. The varactor loop detail is depicted in Figure 2.5. However the physical loop construction is not described in the paper but one can expect that for a reliable and consistent performance, a firm mounting is required. Otherwise the ‘dangling’ loop would give inconsistency coupling to the DR. Even without the varactors being biased, the fluctuation of the loop itself is sufficient to perturb the H-field.

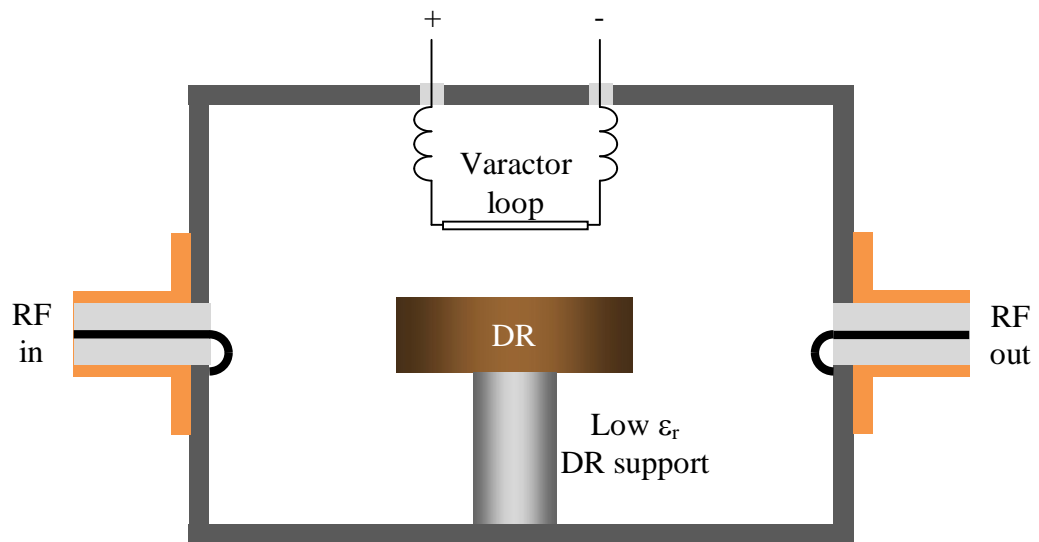


Figure 2.4: Dielectric resonator resonant circuit with balance loop varactor tuning (El-Moussaoui, Kazeminejad et al. 1989).

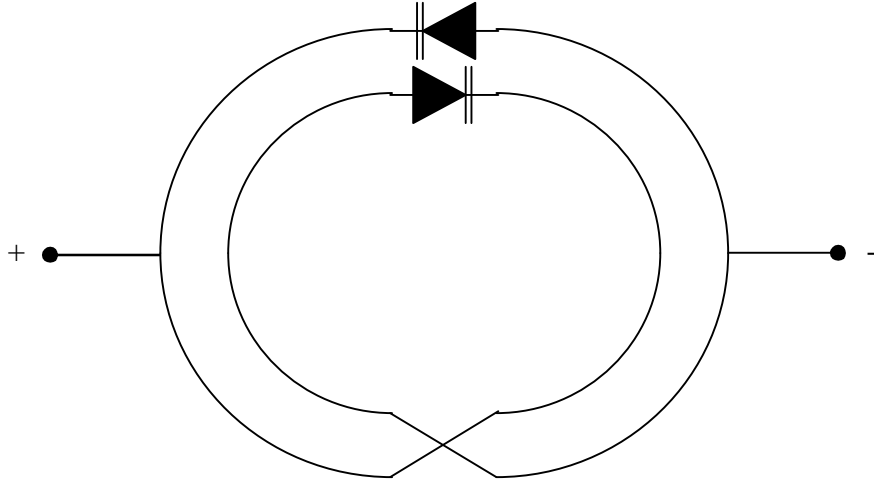


Figure 2.5: Balanced loop varactor circuit (El-Moussaoui, Kazeminejad et al. 1989)

Moussaoui's results however, are interesting for this work as they explain the performance of the DR circuit under weak and strong varactor couplings. Under weak coupling, the tuning range is small, low insertion loss (IL) at resonant frequency and high unloaded Q (Q_U) factor is maintained. Whereas under strong coupling, the tuning range achieved is big but at a cost of high IL at resonant as well as Q_U factor degradation.

2.6.3.2 Tuning by Coupling to a Non-Resonant Microstrip Line

Practically the manufactured DR resonant frequency accuracy comes with a certain tolerance. The one used in this work is specified with ± 18 MHz. With a tuning voltage limited to 10 V for this work, it will require such a high tuning sensitivity to cover more than 36 MHz only to compensate for the tolerance, not to mention the oscillator tuning in phase-locked operation. A passive tuning or adjustment using

three-quarter wavelength microstrip line (Buer and El-Sharawy 1995) can be used to compensate for the DR frequency tolerance. This technique would be convenient because it allows for a planar circuit layout. By adjusting the position of the three-quarter wavelength microstrip line, the amount of H-field perturbation can be controlled and hence the nominal resonant frequency of the DR can be set. The technique is further developed to include varactor for electrical tunability whereby the microstrip line length is reduced to half wavelength with the varactor incorporation. For this method however, since the position of the microstrip line would be different from one circuit to the other, the wiring of the varactor bias cannot be fix too, i.e. it has to follow the position of the microstrip line. This will possibly require fine manual wiring and is undesirable for mass production environment.

As can be seen, DR tuned by varying external reactance (e.g. a photoconductive patch, a varactor or a certain wavelength microstrip line) requires the device to be coupled to a tuning line or stub (El-Moussaoui, Kazeminejad et al. 1989; Buer and El-Sharawy 1995; Virdee 1997; Jianping and Deming 1998). The reactance translates into the TEM mode H-field along the tuning stub that effectively couples to the DR. The tuning stub length determines the tuning range of the DR (Virdee 1997; Xiaoming and Sloan 1999). However the stub length is fixed or patches (very short, e.g. square shape stubs) are added at the one end of the line for limited length adjustment. This is because, due to materials variations, the predetermined tuning stub length may not be optimum to some circuits compared to the others; and thus yields varying results.

2.6.3.3 Secondary Varactor to Optimize Tuning Stub Electrical Length

Xu and Sloan (Xiaoming and Sloan 1999) proposed a more flexible tuning stub adjustment by adding a secondary varactor. The primary varactor, as with other methods discussed earlier is to vary the reactance of the DR. The secondary varactor is to adjust the tuning stub electrical length and hence ensuring the optimum results for each circuit.

Figure 2.6(a) shows the equivalent electrical schematic of Xu's proposed varactor tuned DR circuit, showing only the tuning stub schematic. The primary varactor for resonator tuning is on the right hand side and the secondary varactor for electrical length, i.e. open circuit (OC) adjustment in on the left hand side. Figure 2.6(b) shows the actual circuits with the DR, the two varactors are in Mesa diode package. By measuring the DR maximum tuning range at different electrical lengths; the tuning stub electrical length that gives the widest resonator tuning range can be determined, the detailed results of this experiment is presented in the paper (Xiaoming and Sloan 1999). However, the loading on the DR Q factor must also be considered, therefore a trade-off between tuning range and unloaded Q factor is usually necessary. With this technique, Xu achieved 89 MHz of tuning range at 8 GHz or 1.1%. The addition of the secondary varactor for electrical length optimization on itself is simple; however the complexity is on the control circuit that will set the bias voltage for the varactor and to 'lock' the bias voltage at the set value consistently.

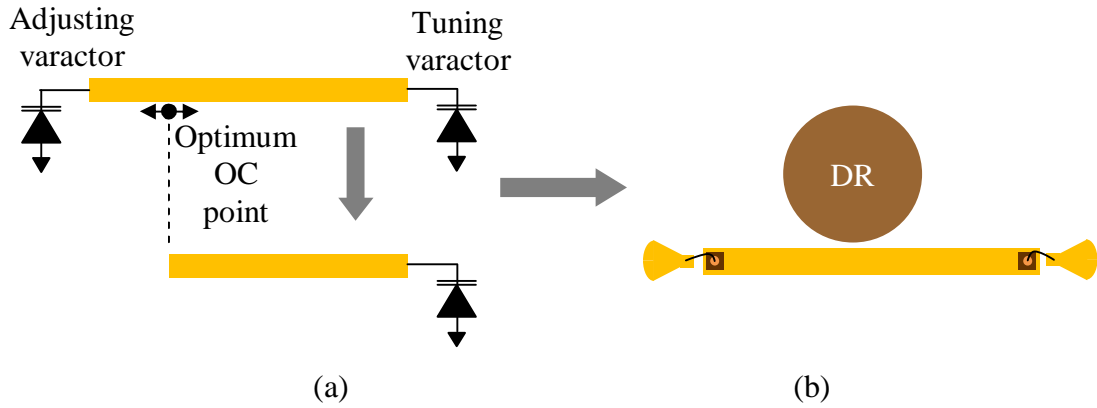


Figure 2.6: Varactor tuning with the tuning stub electrical length optimizable (Xiaoming and Sloan 1999).

2.6.3.4 Circular Tuning Stub

Virdee (Virdee 1997) proposed a rather compact varactor-microstrip tuning stub coupling to the DR by making the microstrip stub circular as shown in Figure 2.7. The loop and the transmission lines dimensions must be determined for optimum tuning range as well as not to degrade the DR Q_U too much. The curvy lines maximize the field couplings. Virdee does not mention whether the loop and the transmission lines dimensions were obtained empirically or by some calculations. The DR is tunable by more than 1.6% or 53.7 MHz at 3.318 GHz with tuning voltage from 0 V to 30 V. The resonant frequency relation with the tuning voltage (or the varactor capacitance) is approximately linear, with this technique. This compact and practical method has a potential and will be further investigated in this work.